JAERI-M
6883

TOTAL NEUTRON CROSS SECTIONS OF LANTHANUM AND PRASEODYMIUM IN THE ENERGY RANGE FROM 20 TO 240 keV

January 1977

K. Nishimura, Y. Yamanouti, S. Kikuchi and T. Nakagawa

日本原子力研究所
Japan Atomic Energy Research Institute

この報告書は，日本原子力研究所がJAERI-Mレポートとして，不定期に刊行している研究報告書です．入手，複製などのお問合わせは，日本原子力研究所技術情報部（茨城県那珂郡東海村）あて，お申しこしください．

JAERI-M reports, issued irregularly, describe the results of research works carried out in JAERI. Inquiries about the availability of reports and their reproduction should be addressed to Division of Technical Information, Japan Atomic Energy Research Institute, Tokai-mura, Naka-gun, Ibaraki-ken, Japan.

JAERI-M 6883

Total Neutron Cross Sections of Lanthanum and Praseodymium in the Energy Range from 20 to 240 keV

Kazuaki NISHIMURA, Yoshimaro YAMANOUTI[+)], Shiro KIKUCHI[+)] and Tsuneo NAKAGAWA[+)]

Radioisotope and Nuclear Engineering School, JAERI

(Received December 23, 1976)

Total neutron cross sections for La and Pr in the energy range from 20 to 240 keV were measured by using monochromatic neutrons, which were produced by the $^{7}Li(p,n)^{7}Be$ reaction. The energy spreads of incident neutrons were about 18 keV for La and about 8 keV for Pr. The measured total neutron cross sections, with statistical error of 2 - 5% for La and 2 - 3% for Pr, were compared with other available data. The average total neutron cross-section data for both nuclides were interpreted in terms of a spherical optical-model potential. S-wave strength functions S_o for La and Pr were deduced from the optical-model parameters obtained by fitting to the average total neutron cross-section data; i.e. $S_o = 0.46 \,^{+\,0.08}_{-\,0.03} \times 10^{-4}$ for La and $S_o = 1.0 \,^{+\,0.15}_{-\,0.08} \times 10^{-4}$ for Pr. The result of total neutron cross sections for La in the energy range from 70 to 140 keV with the energy spreads of about 2.8 keV is also presented.

+) Division of Physics, Tokai, JAERI

20から240 keVのエネルギー範囲における LaとPrの中性子全断面積

日本原子力研究所ラジオアイソトープ・原子炉研修所

西村和明・山内良麿*・菊池士郎*・

中川庸雄*

（ 1976年12月23日受理 ）

LaとPrの中性子全断面積を，単色エネルギーの中性子を使って20から240 keV のエネルギー範囲で測定した。単色エネルギーの中性子は ^{7}Li（p，n）^{7}Be 反応で発生させた。入射中性子のエネルギーの拡がりは，Laの場合約18 keV，Prの場合約8 keVであった。 Laに対して2－5％，Prに対して2－3％の統計誤差で測定された中性子全断面積を，利用できる他の実験データと比較した。両方の核種に対する，平均化された中性子全断面積のデータを，球形光学模型によって解釈した。平均化された中性子全断面積データに適合することによって得られた光学模型パラメーターから，LaとPrに対するS波強度関数S_0を導出した。 すなわち，Laに対して$S_0 = 0.46 \begin{matrix} +0.08 \\ -0.03 \end{matrix} \times 10^{-4}$，Prに対して$S_0 = 1.0 \begin{matrix} +0.15 \\ -0.08 \end{matrix} \times 10^{-4}$ である。 約2.8 keVの入射中性子エネルギーの拡がりで，70から140 keV のエネルギー範囲で測定した，Laの中性子全断面積の測定結果もまた提示している。

*） 日本原子力研究所東海研究所物理部

I. INTRODUCTION

The experimental data of the total neutron cross sections for lanthanum and praseodymium are not numerous in the keV region lower than 250 keV. Miller et al.[1] measured the total neutron cross sections in the energy range from 50 keV to 3.2 MeV with an interest to find gross structure. Their data were sparsely distributed in the lower energy region. The result of Newson et al.[2] showed no remarkable structure in the energy range from 1 to 100 keV for lanthanum, and they reported appearances of fluctuating cross sections for praseodymium in the energy range from 0.5 to 150 keV. The measurement for lanthanum made by Tabony et al.[3] in the energy range from 30 to 650 keV, with the incident energy spread of about 10 keV, indicated rather large fluctuation from 4.1 to 5.5 barns below 200 keV. Wynchank et al.[4] made the measurement for praseodymium from 10 eV up to 340 keV with the time-of-flight method, and obtained resonance parameters below 10 keV. They presented fluctuating cross sections in the lower keV region and smoothly varying cross sections in the higher keV region.

The experimental data of S-wave strength function to be compared with optical model prediction are relatively few in the mass number region around 140, where neutron magic (N=82) nuclei such as ^{139}La and ^{141}Pr are included. Most of the data on the S-wave strength function for these nuclei were deduced from the analysis of individual resonances, except for the data of Seth et al.[5] being deduced from average total neutron cross sections for lanthanum.

In order to provide further experimental data of total neutron cross sections and to deduce the S-wave strength function from fitting to the average total neutron cross sections, the transmission measurements for

lanthanum and praseodymium were performed in the energy range from 20 to 240 keV with the energy spread of about 18 keV for lanthanum and about 8 keV for praseodymium. The average total neutron cross sections obtained from the present transmission measurements were compared with an optical model calculation. From the optical model parameters obtained by fitting to the average total neutron cross sections, S-wave strength functions were deduced for the both nuclides.

The closed-shell nuclei such as ^{139}La and ^{141}Pr behave like lighter nuclei, and the better chance of detection of pronounced fluctuation in the total neutron cross section would be expected for these nuclei at low energies. Thus, another measurement of the total neutron cross section for lanthanum was made to find structure, if any, at the lower energies from 70 to 140 keV with a narrow energy spread of about 2.8 keV. Fluctuating cross sections were observed, and the result is presented in this report.

II. EXPERIMENTAL

The plane view of the experimental arrangement is shown in Fig. 1.

A) Source

Monoenergetic neutrons were produced by using the ^{7}Li(p,n)^{7}Be reaction. The neutrons emitted from the lithium target were collimated by a polyethylene collimator in the direction of $\theta = 100 \pm 1.8^{o}$ with respect to proton beams from the JAERI 5.5-MV Van de Graaff accelerator.

Lithium-fluoride was evaporated onto the molybdenum backing plate of 0.3-mm thickness within the limited area of 5-mm diameters. For the purpose of keeping good vacuum and efficient heat conduction, indium wire of

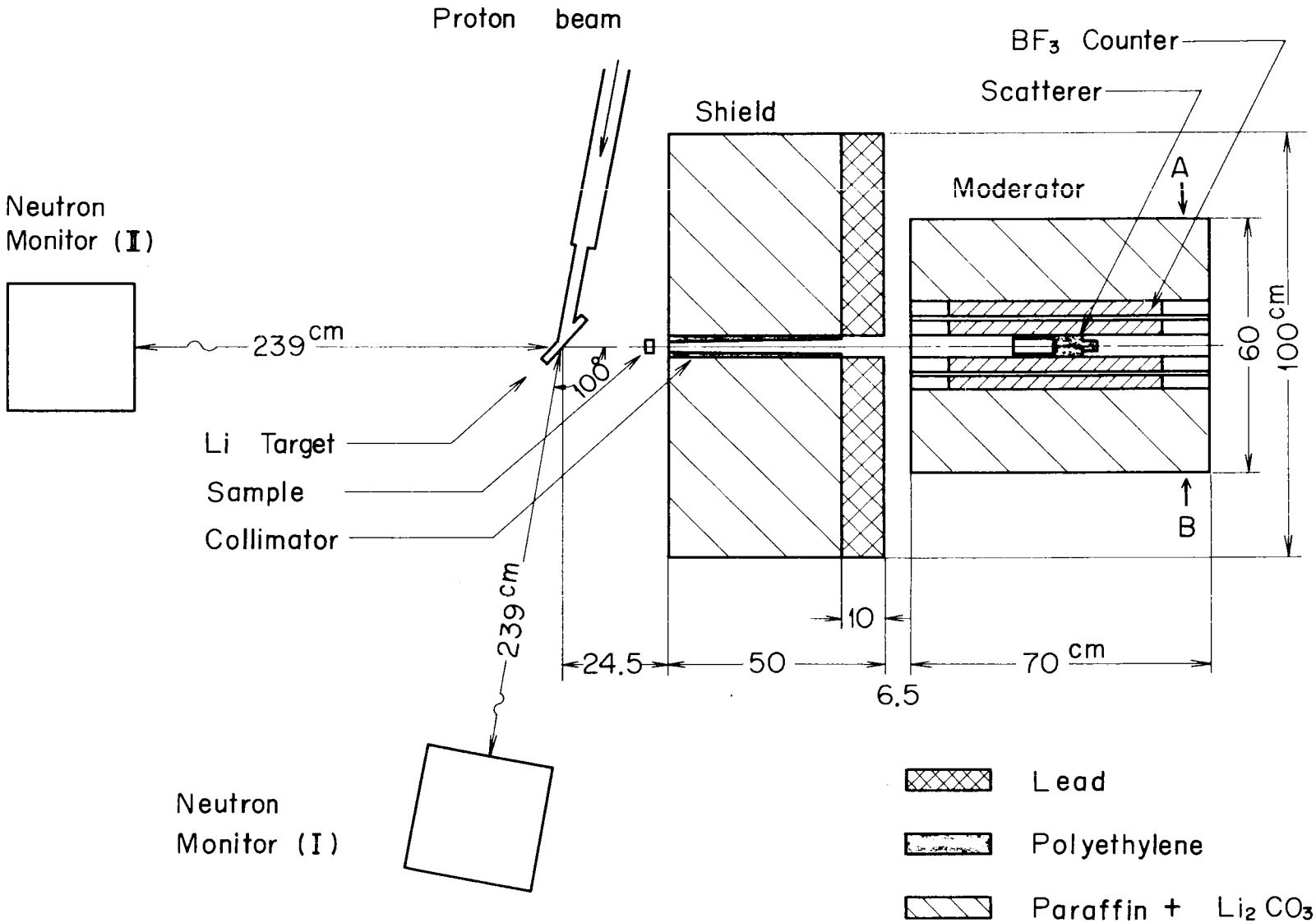

Fig. 1 Plane view of experimental arrangement.

1-mm diameter was used as a gasket. The dimension of the lithium target assembly is presented in Appendix I. The outside of surface of the molybdenum plate was cooled by the jet spray of mist, and no lithium-fluoride ran out during the bombardment of proton beams of about 5 μA.

Neutron energy spreads resulting from the collimator opening of $\pm$ 1.8° were calculated by kinematics of the $^{7}Li(p,n)^{7}Be$ reaction, and the spreads were $\pm$ 1.1, $\pm$ 2.8 and $\pm$ 4.1 keV at neutron energies of 15, 80 and 150 keV, respectively. In order to determine the thickness of the lithium target experimentally, two different methods were used; i.e. a rise-curve method at threshold[6] and a time-of-flight technique[7]. The two estimations of the incident neutron energy spread based on the above methods were in good agreement within experimental error of about 5%. Experimental procedure and a typical result are presented in Appendix II. The neutron energy spreads (full width at half maximum) thus obtained were about 18 keV for the measurement of lanthanum, and about 8 keV for praseodymium.

B) Collimator and shield

The length and outer diameter of the polyethylene collimator was 40.8 cm and 4.4 cm. The inner diameters of the collimator were 1.57 cm and 4.18 cm at the front and rear edges, respectively. The distance from the lithium target to the front edge of the collimator was fixed at 24.5 cm.

The polyethylene collimator was inserted into a 3-mm thick copper pipe, which was of 40 cm in length and 4.4 cm in inner diameter. The copper pipe was embedded in a paraffin neutron shield. The dimension of the paraffin neutron shield is shown in Fig. 1. A 10-cm thick layer of lead was attached at the rear side of the neutron shield.

C) Detector

A neutron detector assembly was placed behind the paraffin neutron

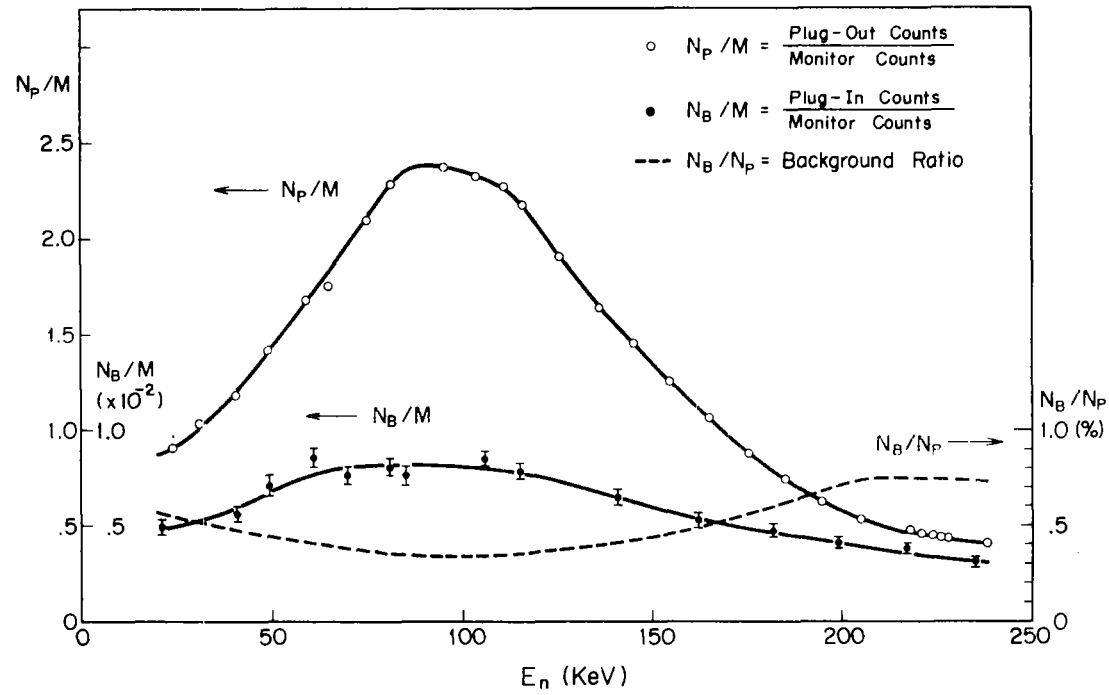

Fig. 2 Measurement of background neutrons. Plug-in counts N_B and plug-out counts N_P were measured as a function of incident neutron energies. The ratios of N_B/N_P were an order of 0.3 - 0.8% in the whole range of neutron energy. The dotted curve was used for the estimation of background neutrons, where the plug-in counts N_B were assumed to be the same as the background counts N_b in the transmission measurement.

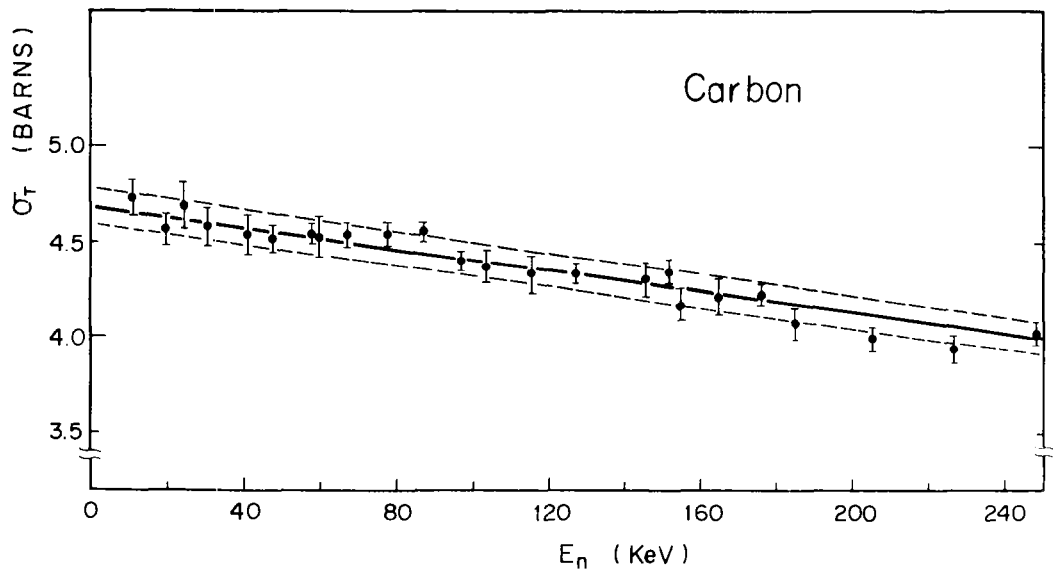

Fig. 3 The total neutron cross sections of carbon obtained with the present procedure. The measurement was carried out to check applicability of the present procedure. The solid curve shown is an evaluated cross-section curve[9]. The dashed curves represent cross-section curves of ± 2% deviation from the evaluated cross-section curve.

shield. The detector assembly consisted of twelve Hitachi BF_3 counters, a polyethylene scatterer and a paraffin moderator. The Hitachi EB-125 BF_3 counter was of 2.65 cm in diameter and 20.5 cm in effective length, and contained 96% enriched $^{10}BF_3$ gas of 500 Torr.

Twelve BF_3 counters were divided into two groups, and the two groups corresponded to two electronic circuit systems. In the electronic circuit system, the pulses from the six BF_3 counters were added, amplified and fed into a fast scaler. The neutrons scattered by the polyethylene scatterer placed at the center of the detector system were moderated by the paraffin moderator and detected by the twelve BF_3 counters. The A-B section of the detector assembly shown in Fig. 1 and the dimension of the polyethylene scatterer are presented in detail in Appendix III.

D) Samples

The samples studied were metallic cylinders of the following geometrical sizes : 1.20 cm in length and 2.50 cm in diameter for lanthanum, and 2.01 cm in length and 2.50 cm in diameter for praseodymium. The sample thicknesses of lanthanum and praseodymium were 0.0328 $X10^{24}$ atoms/cm^2 and 0.0580 $X10^{24}$ atoms/cm^2, and gave average transmissions of about 0.86 and about 0.75, respectively. The sample purities of both elements were 99% and 99.9%. The both natural elements are nearly monoisotopic (^{139}La, 99.91%) and monoisotopic (^{141}Pr, 100%), respectively.

E) Procedure

The samples were mounted on a remote control sample changer and were placed at the front of the polyethylene collimator. The counts with the sample in place and the counts with no sample were measured alternatively, until the total counts in the respective runs of sample-in and sample-out amounted to more than 40,000 counts. Then the total neutron cross section

σ_T and its statistical error $\Delta\sigma_T$ were estimated from the following formulas :

$$\sigma_T = (1/n)\ln(1/T) \quad \text{and} \quad \Delta\sigma_T/\sigma_T = (\Delta T)/(T.\ln T) \qquad (1),$$

where n is a sample thickness in atoms/cm^2 and T is transmission, i.e. $T = (N_I - N_b)/(N_o - N_b)$. Here, N_I, N_o and N_b are sample-in, sample-out and background counts, respectively. These counts were normalized to the monitor counts, M. The background counts N_b in the sample-in and sample-out measurements were assumed to be equal.

The background measurement was carried out by plugging the hole of the copper pipe with a polyethylene solid cylinder of 26.5-cm long and 4.4-cm diameter. The counts with the plug (plug-in counts, N_B) and the counts without the plug (plug-out counts, N_P) were measured as a function of incident neutron energies. The results of N_B and N_P are shown in Fig. 2 by closed and open circles, respectively. The percentage of the plug-in counts to the plug-out counts, i.e. the ratios of N_B/N_P, were an order of 0.3 - 0.8% in the whole neutron energy range, as shown by dashed curve in Fig. 2. The plug-in counts N_B were assumed to be the same as the background counts N_b in this experiment, and they were estimated from the curve of N_B/M in Fig. 2.

Correction for single inscattering by the sample into the collimator was estimated using a formula similar to that quoted by Miller[8]. The effect of inscattering was about 0.12%, indicating appropriateness of the present geometry, and no correction for inscattering was applied to the data.

F) Measurement of the total neutron cross section of carbon

In order to check the experimental apparatus and procedure for the present work, especially propriety for the estimation of the background

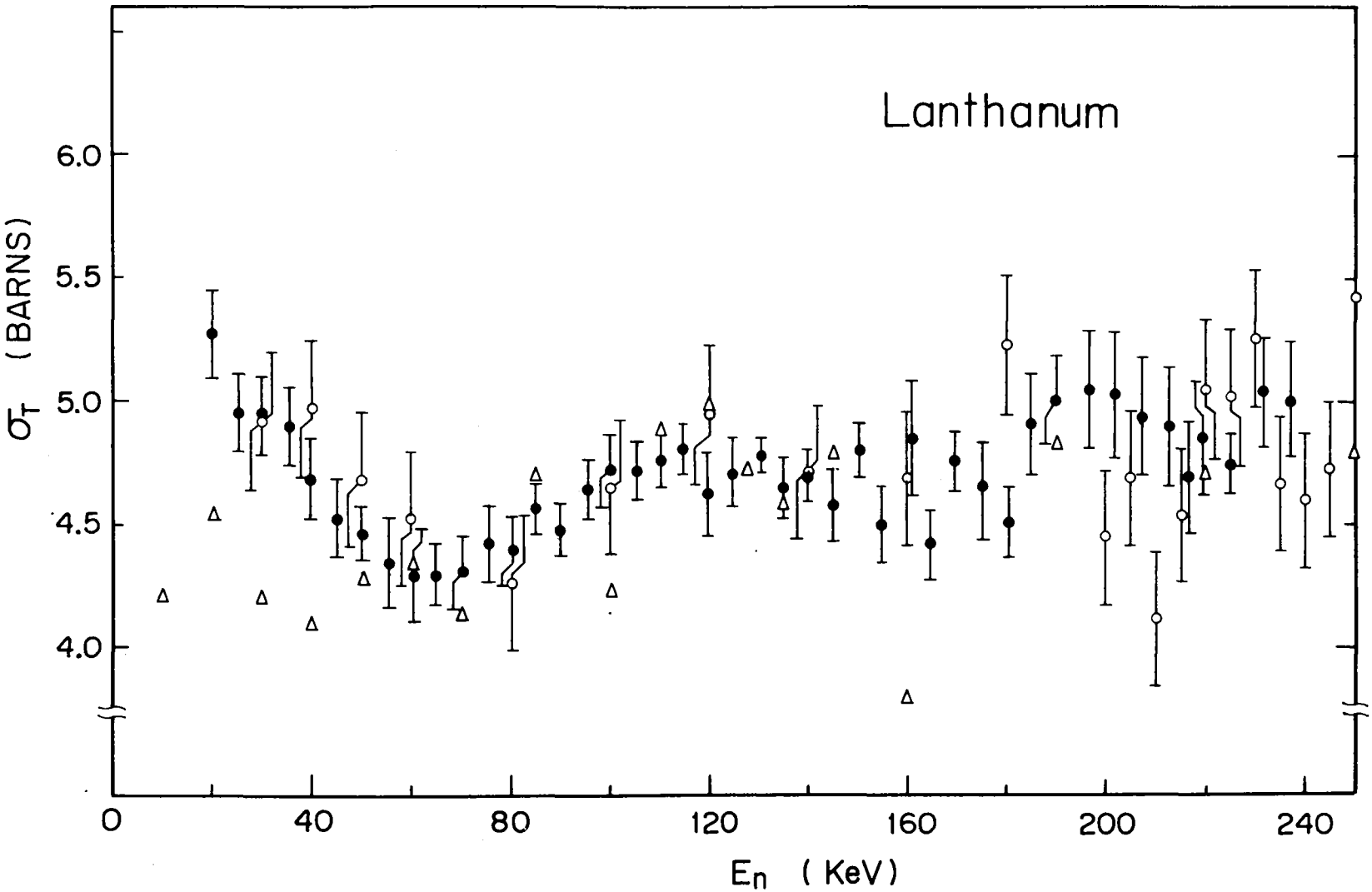

Fig. 4 The present result of total neutron cross sections for lanthanum is shown by closed circles, where the energy spread of neutrons is 18 keV. The results of Miller et al.[1] and Tabony et al.[3] are shown by open triangles and open circles, respectively.

counts N_b, the total neutron cross section of carbon was measured in the neutron energy range from 10 to 250 keV. The neutron energy spread used was about 5 keV. The size of the carbon sample was 2.50 cm in diameter and 1.18 cm in thickness, and its quality was of reactor grade. The sample thickness was 0.094 $X10^{24}$ atoms/cm^2, and the transmission was the order of about 0.68.

The result of the total neutron cross-section measurement for carbon, which was obtained by the experimental procedure mentioned in E), is shown in Fig. 3 by the closed circles. The solid curve in Fig. 3 indicates an evaluated cross section curve for carbon[9]. The dashed curves indicate the $\pm$ 2% deviation from the evaluated cross-section curve. The result of the measurement was in good agreement with the evaluated cross-section curve within the statistical error of about 1.7%. It was, therefore, ascertained that the present experimental procedure and apparatus were reasonably applicable for the measurement of the total neutron cross section with about 2% of systematical uncertainty.

III. RESULTS

The measured total neutron cross sections for lanthanum and praseodymium are plotted by the closed circles in Figs. 4 and 5. The data of Wisconsin[1] and Duke[3] are also shown in the figures by open triangles and open circles, respectively. The statistical error was estimated to be $\pm$ 2 - 5% for lanthanum and $\pm$ 2 - 3% for praseodymium, and it is shown by error bars in the figures. The present results for lanthanum and praseodymium, as well as for carbon are listed in Table I.

The present results for lanthanum and praseodymium were corrected

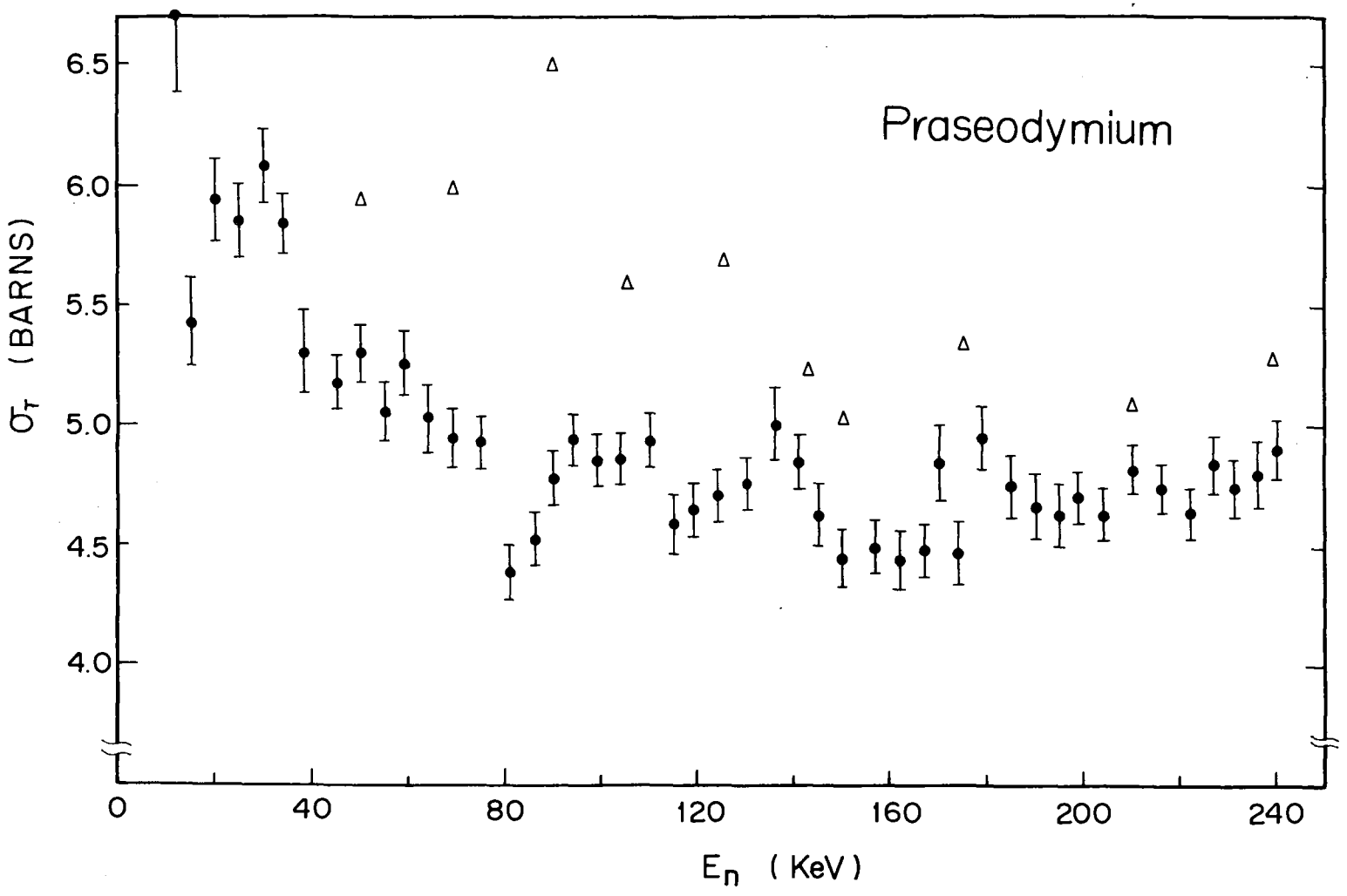

Fig. 5 The present result of total neutron cross sections for praseodymium is shown by closed circles, where the energy spread of neutrons is 8 keV. The present cross-section values are systematically lower (about 10 to 20%) than those of Miller et al.[1], which are shown by open triangles.

for sample thickness, especially at lower energies. Doppler width, average reduced neutron width $\langle \Gamma_n^o \rangle$, average level spacing $\langle D \rangle$ and potential scattering radius R' were needed for the correction. These values for both nuclei were taken from BNL 325 3rd edition[10]. The correction for sample thickness was estimated to be 2.1% for lanthanum and 5.3% for praseodymium at the neutron energy of 30 keV by using a simple model of resonances[11]. Due to the 1/E variation in the resonance peak cross section, the correction decreased to less than 1% above 36 keV for lanthanum and above 80 keV for praseodymium.

The present result for lanthanum shown in Fig. 4 was in good agreement with Duke's one[3] below 160 keV. Both results indicate variation with the width of about 40 keV. The agreement of the present result with Wisconsin's one[1] was not so good below 40 keV and at 160 keV.

The present cross-section values for praseodymium plotted in Fig. 5 show systematically lower values than Wisconsin's data[1]. Their data were higher by about 1.1 barns (20%) below 120 keV and 0.5 barns (10%) above 140 keV. In order to check reliability of our data, transmissions were remeasured at 15, 30, 140, 180 and 235 keV with about same energy spreads of 6.0 and 8.2 keV as before. Thus, it was confirmed that the previous cross-section values were reproduced within statistical error of 2 - 3%.

The present data for praseodymium were also compared with the time-of-flight measurement of Wynchank et al.[4], which indicated much resonances in the lower energy region. A fairly good agreement was obtained above 35 keV between both measurements, although our data were sparsely distributed in the energy region compared.

In the case of lanthanum, another measurement for the total neutron

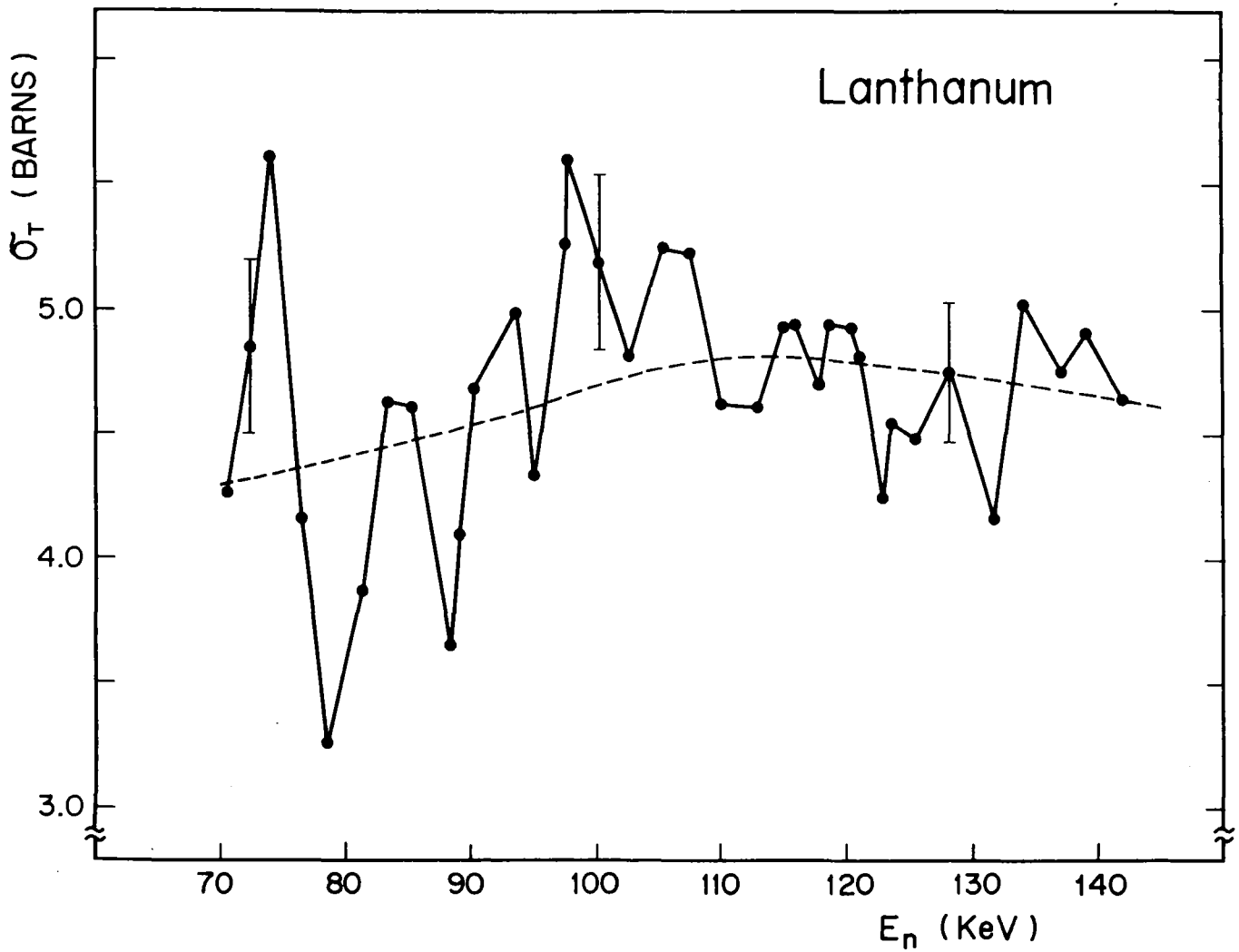

Fig. 6 The result of total neutron cross sections for lanthanum in the energy region from 70 to 140 keV, measured with the smaller energy spread of neutrons of about 2.8 keV. The solid curve indicates fluctuation of the measured cross sections, and the dashed curve represents a part of the cross section curve drawn through the experimental data of Fig. 4.

cross section was performed to find fluctuating behaviour with a narrower energy spread. The choice of lanthanum was made due to its smaller binding energy (E_b=5.161 MeV) and, hence, its larger average spacing ($\langle D \rangle$ = 0.24 keV) compared to those values (E_b=5.844 MeV and $\langle D \rangle$ =75 eV) of praseodymium. The result of the measurements with the thin Li targets of about 2.8 keV is shown by closed circles in Fig. 6, and the numerical data is listed in Table II. The result obtained by the thick targets of about 18 keV is also shown in Fig. 6 with a dashed curve. In fact, marked fluctuation is observed as compared with the dashed curve, even though the statistical error of the fluctuating cross section was relatively large (about $\pm$ 7%) due to low intensity of the incident neutron flux.

The fluctuation observed might be explained as statistical fluctuation of the compound nucleus level density for ^{140}La at excitation energies from 5.231 MeV to 5.301 MeV. The energy range of excitation studied was rather small to make a significant average, so that auto-correlation analysis was not applied to the observed structure. At the present time, no explanation we can give about the nature of the observed structure.

IV. COMPARISON WITH OPTICAL MODEL CALCULATION

The energy spreads in the incident neutron beams were about 18 keV for lanthanum and 8 keV for praseodymium. It was hoped that such spreads might be sufficient to provide an energy average over the resonances in the compound systems of both the magic neutron nuclei. However, structure was actually observed in the measured total neutron cross sections, as shown in Figs. 4 and 5. Even though the optical model cannot reproduce such structure, it is interesting to see how accurately this model can

describe the average behaviour of the total neutron cross sections, especially in the keV region lower than 250 keV.

In order to compare with the optical model calculation, it is reasonable to use average smoothed cross sections rather than measured fluctuating cross sections. The average cross sections $\bar{\sigma}(E)$ were obtained from the measured cross sections $\sigma(E)$ by the use of AVERAGE code[12], in which the average cross section $\bar{\sigma}(E)$ was defined as

$$\bar{\sigma}(E) = \frac{1}{\Delta E} \int_{E-\frac{1}{2}\Delta E}^{E+\frac{1}{2}\Delta E} \sigma(E)dE \qquad (2).$$

Here, ΔE is the energy width of the average.

Three different values of ΔE, i.e. 50, 75 and 100 keV, were tentatively chosen to see the change of smoothness on the calculated cross section curve of $\bar{\sigma}(E)$. No appreciable difference was found in the both shapes of $\bar{\sigma}(E)$, being calculated with ΔE=75 keV and ΔE=100 keV. Then, ΔE=75 keV was finally adopted in the present calculation. It is noted that actually a smaller value of ΔE than 75 keV was taken at the both energy regions of $E_1 < E < E_1$+75 keV and E_2-75 keV$< E < E_2$, where E_1 and E_2 denotes the lowest and highest incident energy of neutrons in the measured cross sections $\sigma(E)$, respectively. The average cross sections $\bar{\sigma}(E)$ thus obtained are presented in Figs. 7 and 8 by the dashed curves of A.

An optical model code TOTAL[13] was used to calculate total neutron cross sections. The optical model potential V_c used in this work was the following :

$$V_c = - V_o f(r) - iW_s g(r) + V_{so}\left(\frac{\hbar}{\mu C}\right)^2 \vec{\sigma}\vec{\ell}\,\frac{1}{r}\cdot\frac{df(r)}{dr} \qquad (3),$$

$$f(r) = [\ 1 + \exp\{(r - R_o)/a\}]^{-1},$$

$$g(r) = 4\ \exp\{(r - R_s)/b\}/[\ 1 + \exp\{(r - R_s)/b\}]^2.$$

Here, V_o and W_s are the real and imaginary potential depths, V_{so} is the spin-orbit potential depth, a and b are the diffuseness of the nuclear surface for the real and imaginary potential well.

Calcualtions of automatic parameter search for V_o and W_s were performed on FACOM 230-60 computer by the use of TOTAL code[13] with χ^2-fitting to the average cross sections $\bar{\sigma}(E)$ obtained above. The values of R_o and R_s were fixed to $R_o=R_s=1.275$ fm by taking into account the results[14], which had been obtained by Fission Product Working Group of the JNDC. The value of V_{so} was fixed at 7.0 MeV. The diffuseness parameters a and b were also fixed as 0.62 fm and 0.227 fm, respectively. The latter value is equivalent to 0.50 fm of diffuseness in Gaussian type potential. These values of the diffuseness parameters are the same as used in the works of Moldauer[15], Engelbrecht and Fiedeldy[16] and Malan et al.[17]

The following energy dependence of the optical model potential was adopted in the present automatic parameter-search calculation, as used in the refence 14, i.e.

$$V_o = V - 0.25E(\mathrm{MeV}) \qquad \text{and} \qquad W_s = W - 0.20E(\mathrm{MeV}) \qquad (4).$$

As the initial values for V and W in equation (4), V=46 MeV and W=14 MeV were taken from the work of Moldauer[15]. The results of automatic parameter search for V and W, which gave a minimum value of χ^2 in fitting to the average cross sections $\bar{\sigma}(E)$, were V=45.25 MeV and W=9.81 MeV for lanthanum, and V=45.88 MeV and W=15.33 MeV for praseodymium. The large difference in imaginary potential W for such neighbouring nuclei is consistent with the fact of rapid rise of S-wave strength function in this mass number region.

The total neutron cross section curves for lanthanum and praseodymium calculated from the sets of potential parameters, in which the above final values of V and W were included, are shwon by the solid curves marked with 1 in Figs. 7 and 8, respectively. The upper and lower curves marked with 2 and 3 in the same figures give a measure of ± 5.2% deviation from the curves marked with 1 at the neutron energy of 100 keV. This deviation corresponds to ± 0.24 barns in the case of lanthanum and ± 0.25 barns in the case of praseodymium.

At first, the upper and lower cross-section values having ± 5% deviation were tentatively adopted at the neutron energies of 50, 100, 150 and 200 keV by taking maximum experimental error of 5% into account. So as to pass the upper and lower curves through around the tentative cross-section values, a series of optical-model calculation was extensively performed by changing the values of V and W, which were not so much different from those of the curve 1. In this calculation, the dependence of the shape and absolute value of the cross-section curve on the values of V and W were systematically taken into account.

Among a series of calculated cross-section curves, the upper and lower curves indicated in Figs. 7 and 8 were finally determined; where the χ^2-value of the curve 2 was chosen to be equal to that of the curve 3. The potential depth parameters V and W corresponding to the cross-section curves 1, 2 and 3 are shown in the inserted tables in Figs. 7 and 8.

In the TOTAL code, transmission coefficent $T_{l=o}$ for S-wave neutrons can be calculated from a set of optical potential parameters, i.e. V, W, V_{so}, R_o, R_s, a and b, and the S-wave strength functions S_o is deduced from the formula of $S_o = T_{l=o}/2\pi\sqrt{E(eV)}$. The results of S_o corresponding

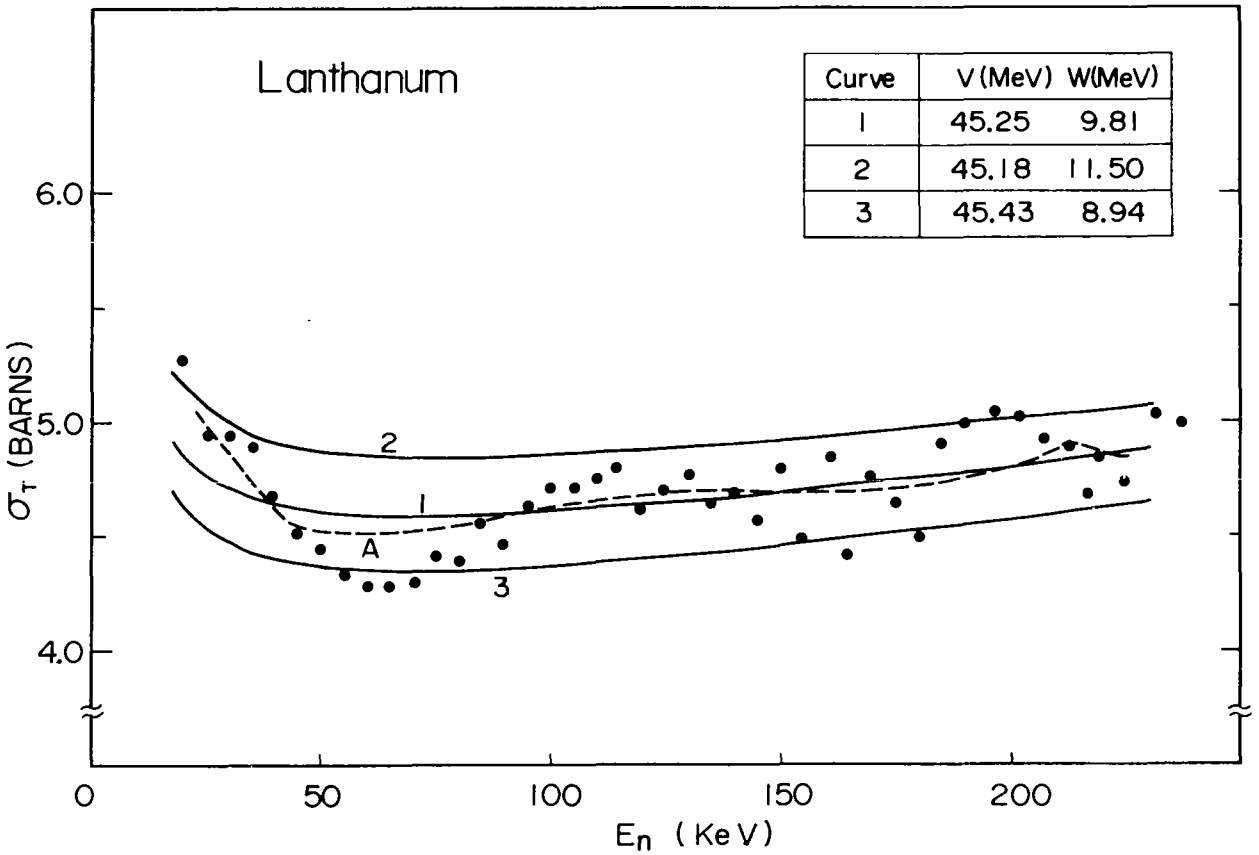

Fig. 7 A comparison of the average total neutron cross-section curve A (dashed curve) for lanthanum with the cross-section curves of 1, 2 and 3 obtained by optical model calculation. The cross-section curve of 1, which gives a minimum χ^2-value, was determined by automatic parameter search for potential depth parameters V and W, by using the TOTAL code to fit the average total neutron cross-section curve A. The upper and lower cross-section curves of 2 and 3, which have about same χ^2-value, give a measure of ±5.2%-deviation from the cross-section curve 1 at the energy of 100 keV. The values of V and W, by which the curves of 1, 2 and 3 were calculated, are shown in the inserted table.

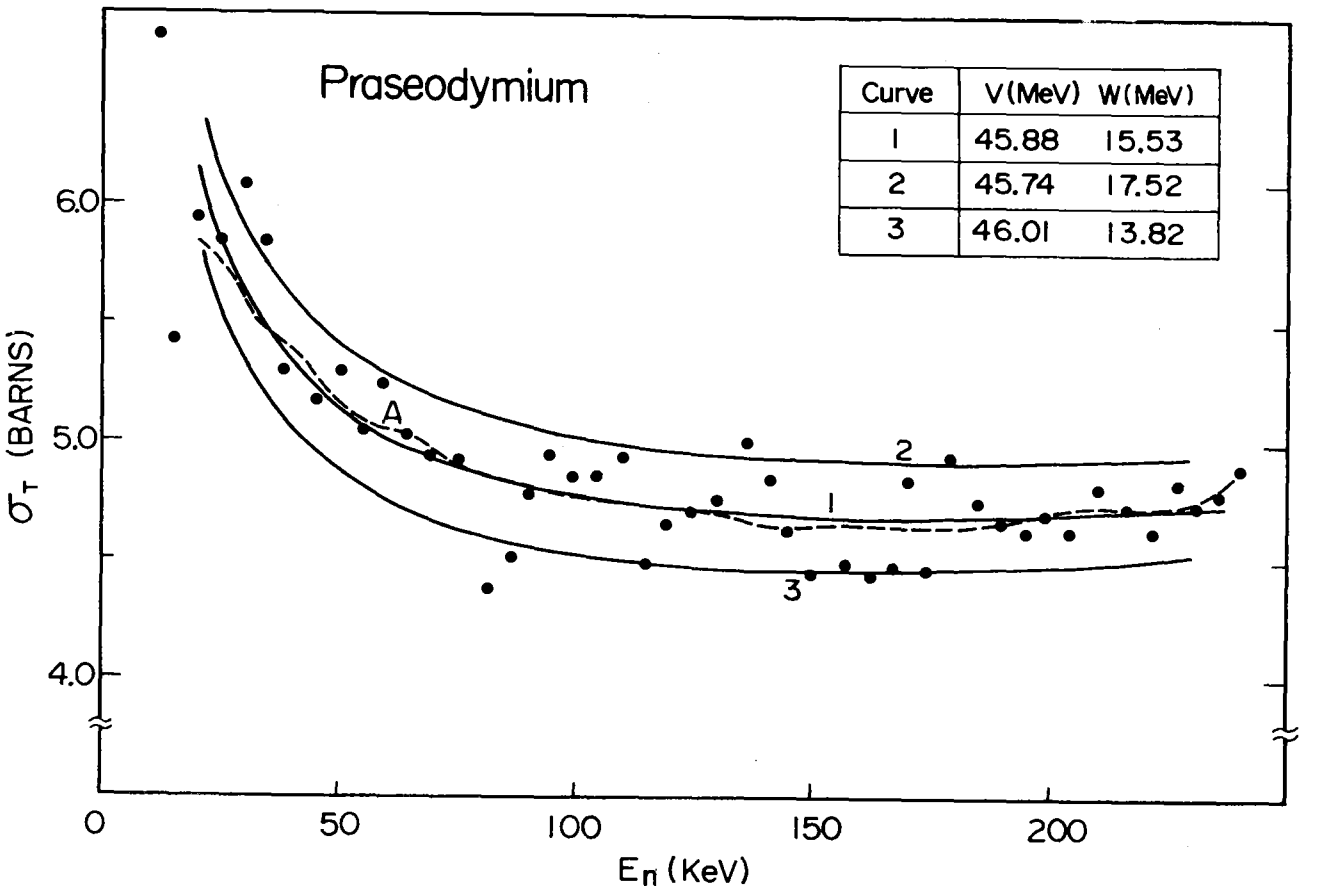

Fig. 8 A comparison of the average total neutron cross-section curve A (dashed curve) for praseodymium with the cross-section curves of 1, 2 and 3 obtained by optical model calculation. Further explanation is the same as in Fig. 7.

to the curves of 1 in Figs. 7 and 8 at E=100 keV were S_o=0.46 X10^{-4} for lanthanum and S_o=1.0 X10^{-4} for praseodymium, respectively. The variations of S_o-values depending upon the neutron energy from 20 to 240 keV were less than 4% for lanthanum, and less than 8% for praseodymium.

In order to estimate uncertainty of S_o, the measure of $\pm$ 5.2% deviation from the curve 1 was chosen in this work. The choice of this deviation resulted in the fact that about 80% of the present data obtained were included in between two curves of 2 and 3. The upper and lower values of S_o were estimated by the use of the optical potential parameter sets, which corresponded to the curves of 2 and 3 in Figs. 7 and 8. The results were $\left(\begin{smallmatrix} +0.08 \\ -0.03 \end{smallmatrix} \right)$X10^{-4} for lanthanum and $\left(\begin{smallmatrix} +0.15 \\ -0.08 \end{smallmatrix} \right)$X10^{-4} for praseodymium, respectively. The choice of the curve 2 and 3 was rather arbitrary; so that problem remains for consideration in the present method of estimation on S_o-uncertainty.

The values of S_o and their uncertainties obtained are presented in Table III, together with those obtained by other authors[4),5),10),18),19)]. The present values of S_o deduced for lanthanum is in agreement with those of other authors within the estimated error. While, the present one for praseodymium indicates about 40% lower value than those obtained by the analysis of individual resonances at eV energies. The parameters of the potential well may be different for S- and P-wave strength functions[20),21)]. Therefore, the optical-model calculations for P-wave strength function could not be carried out simultaneously with the same potential parameter sets as used in the calculation of S-wave strength functions.

Acknowledgement

The authors are indebted to Dr. S. Igarasi for making use of the TOTAL code before his publication and for fruitful discussions on optical model calculation. Helpful discussion on the sample thickness correction with Professor R.C. Block is gratefully acknowledged. The authors wish to thank Drs. S. Tanaka and T. Fuketa for their careful reading and comments on the manuscript. Acknowledge is also due to Messrs. Y. Sato and T. Yoshida for their help with the experiment and for their operation of the 5.5-MV Van de Graaf accelerator.

References

(1) Miller, D.W., Adair, R.K., Bockelman, C.K. and Darden, S.E.: Phys. Rev. 88, 83 (1952).

(2) Newson, H.W., Gibbons, J.H., Marshak, H., Williamson, R., Mobley, R.C., Patterson, J.R. and Nichols, P.F.:Phys. Rev. 105, 198 (1957).

(3) Tabony, R.H., Seth, K.K. and Bilpuch, E.G.:BNL 325 Second Edition Suppl., No.2 May (1966); Annals of Physics 46, 401 (1968).

(4) Wynchank, S., Garg, J.B., Havens, Jr., W.W. and Rainwater, J.: Phys. Rev. 166, 1234 (1968).

(5) Seth, K.K., Tabony, R.H., Bilpuch, E.G. and Newsons, H.W.: Physics Letters 13, 70 (1964).

(6) Gibbons, J.H. and Newson, H.W.:Fast Neutron Physics, Part I, P.133 (1960).

(7) Schwarz, S. and Stromberg, L.G.:Nucl. Inst. Meth. 27, 332 (1964).

(8) Miller, D.W.:Fast Neutron Physics, Part II, P.985 (1963).

(9) Nishimura, K., Igarasi, S., Fuketa, T. and Tanaka, S.:JAERI 1218 (1971).

(10) BNL 325 Third Edition, Vol. 1 June (1973).

(11) Block, R.C.:Private communication.

(12) Nakagawa, T.:Private communication.

(13) Igarasi, S., Nakagawa, T. and Kawai, M.:Private communication.

(14) Igarasi, S. et al.:JAERI-M 5752 (1974).

(15) Moldauer, P.A.:Nucl. Phys. 47, 65 (1963).

(16) Engelbrecht C.A. and Fiedeldey, H.:Annals of Physics 42, 262 (1967).

(17) Malan, J.G., Mcmurray, P., Van der Merwe, P., Van Heerden, I.J. and Engelbrecht, C.A. : Nucl. Phys. A 124, 111 (1969).

(18) Hla Shwe, Cote, R.E. and Prestwich, W.V. : Phys. Rev. 159, 1050 (1967).

(19) Mörgenstern, J., Alves, R.N., Julien, J. and Samour, C. : Nucl. Phys. A 123, 561 (1969).

(20) Jain, A.P., Chrien, R.E., Moore, J.A. and Palensky, H. : Phys. Rev. 137, B83 (1965).

(21) Camarda, H.S.: Phys. Rev. C 9, 28 (1974).

Table I. Present Results of Total Neutron Cross Sections for La, Pr and C.

1) Lanthanum

E_n(keV)	$\sigma \pm \Delta\sigma$(barns)	E_n(keV)	$\sigma \pm \Delta\sigma$(barns)
20	5.27 ± 0.18	145	4.58 ± 0.15
26	4.95 ± 0.16	150	4.80 ± 0.11
30	4.94 ± 0.16	155	4.50 ± 0.15
35	4.89 ± 0.16	161	4.85 ± 0.24
40	4.68 ± 0.17	165	4.43 ± 0.14
45	4.52 ± 0.16	170	4.76 ± 0.12
50	4.46 ± 0.11	175	4.64 ± 0.20
55	4.34 ± 0.18	180	4.51 ± 0.14
60	4.29 ± 0.19	185	4.91 ± 0.21
65	4.29 ± 0.13	190	5.01 ± 0.18
70	4.30 ± 0.15	197	5.05 ± 0.24
75	4.42 ± 0.16	202	5.03 ± 0.25
80	4.39 ± 0.14	207	4.94 ± 0.24
85	4.56 ± 0.10	213	4.90 ± 0.24
90	4.48 ± 0.11	216	4.70 ± 0.22
95	4.64 ± 0.12	219	4.85 ± 0.23
100	4.72 ± 0.15	225	4.75 ± 0.12
105	4.72 ± 0.12	232	5.04 ± 0.22
110	4.76 ± 0.10	237	5.01 ± 0.23
115	4.81 ± 0.10		
120	4.62 ± 0.17		
125	4.71 ± 0.14		
130	4.78 ± 0.10		
135	4.65 ± 0.12		
140	4.70 ± 0.10		

2) Praseodymium

E_n(keV)	$\sigma \pm \Delta\sigma$(barns)	E_n(keV)	$\sigma \pm \Delta\sigma$(barns)
20	5.94 ± 0.17	145	4.63 ± 0.13
25	5.85 ± 0.15	150	4.45 ± 0.12
30	6.08 ± 0.15	157	4.50 ± 0.11
34	5.84 ± 0.12	162	4.44 ± 0.12
38	5.30 ± 0.16	167	4.48 ± 0.11
45	5.18 ± 0.11	170	4.85 ± 0.16
50	5.30 ± 0.12	174	4.47 ± 0.13
55	5.06 ± 0.12	179	4.95 ± 0.13
59	5.26 ± 0.13	185	4.75 ± 0.13
64	5.03 ± 0.14	190	4.67 ± 0.13
69	4.95 ± 0.12	195	4.63 ± 0.13
75	4.93 ± 0.11	199	4.70 ± 0.11
81	4.39 ± 0.11	204	4.63 ± 0.11
86	4.53 ± 0.11	210	4.82 ± 0.10
90	4.78 ± 0.11	216	4.74 ± 0.10
94	4.95 ± 0.11	222	4.64 ± 0.11
99	4.86 ± 0.11	227	4.84 ± 0.12
104	4.86 ± 0.11	231	4.74 ± 0.12
110	4.94 ± 0.11	236	4.80 ± 0.14
115	4.49 ± 0.12	240	4.90 ± 0.12
119	4.65 ± 0.11		
124	4.71 ± 0.11		
130	4.76 ± 0.11		
136	5.01 ± 0.15		
141	4.85 ± 0.11		

3) Carbon

E_n(keV)	$\sigma \pm \Delta\sigma$ (barns)	E_n(keV)	$\sigma \pm \Delta\sigma$ (barns)
11	4.73 ± 0.09	146	4.30 ± 0.09
19	4.57 ± 0.08	152	4.34 ± 0.06
24	4.69 ± 0.12	155	4.17 ± 0.08
31	4.58 ± 0.10	165	4.21 ± 0.09
41	4.54 ± 0.10	176	4.22 ± 0.05
47	4.52 ± 0.07	185	4.07 ± 0.08
58	4.54 ± 0.05	205	3.99 ± 0.06
60	4.53 ± 0.11	227	3.94 ± 0.07
67	4.54 ± 0.06	249	4.02 ± 0.06
78	4.40 ± 0.06		
87	4.56 ± 0.05		
97	4.40 ± 0.05		
104	4.37 ± 0.09		
115	4.33 ± 0.10		
127	4.33 ± 0.05		

Table II. Present Result of Total Neutron Cross Section for La, with the thin targets of about 2.8 keV.

E_n(keV)	$\sigma \pm \Delta\sigma$(barns)	E_n(keV)	$\sigma \pm \Delta\sigma$(barns)
70.6	4.26 ± 0.39	112.9	4.61 ± 0.31
72.2	4.85 ± 0.35	115.3	4.93 ± 0.35
73.9	5.61 ± 0.39	116.1	4.94 ± 0.27
76.3	4.16 ± 0.39	117.9	4.71 ± 0.27
78.8	3.26 ± 0.39	118.6	4.94 ± 0.38
81.5	3.87 ± 0.39	120.3	4.93 ± 0.27
83.5	4.63 ± 0.30	121.1	4.81 ± 0.39
85.2	4.61 ± 0.32	123.0	4.25 ± 0.32
88.4	3.65 ± 0.27	123.7	4.55 ± 0.38
88.9	4.10 ± 0.39	125.4	4.49 ± 0.33
90.1	4.69 ± 0.30	128.1	4.76 ± 0.29
93.9	4.99 ± 0.32	131.8	4.16 ± 0.45
95.1	4.34 ± 0.32	133.9	5.01 ± 0.39
97.6	5.27 ± 0.39	137.0	4.75 ± 0.39
97.8	5.60 ± 0.32	139.5	4.91 ± 0.37
100.1	5.19 ± 0.35	142.1	4.64 ± 0.40
102.8	4.82 ± 0.27		
105.2	5.41 ± 0.38		
107.8	5.23 ± 0.31		
110.2	4.63 ± 0.35		

Table III. S-wave Strength Functions S_o for La and Pr.

	S_o ($X10^{-4}$)	Energy range	References
La	0.75 ± 0.25	30-650 keV	Seth et al.[5]
	$0.7\ ^{+\ 1.0}_{-\ 0.3}$	0.1 eV-1 keV	Hla Shme et al.[18]
	$0.70\ ^{+\ 0.20}_{-\ 0.14}$	0-5.6 keV	Morgenstern et al.[19]
	0.6 ± 0.2		BNL 325 Third Ed.[10]
	$0.46\ ^{+\ 0.08}_{-\ 0.03}$	20-240 keV	Present work
Pr	1.72 ± 0.25	0-10 keV	Wynchank et al.[4]
	$2.04\ ^{+\ 0.47}_{-\ 0.35}$	0-5.7 keV	Morgenstern et al.[19]
	1.72 ± 0.25		BNL Third Ed.[10]
	$1.0\ ^{+\ 0.15}_{-\ 0.08}$	20-240 keV	Present work

APPENDIX

I. Dimension of the 100°-lithium target assembly is shown in Fig. 9.

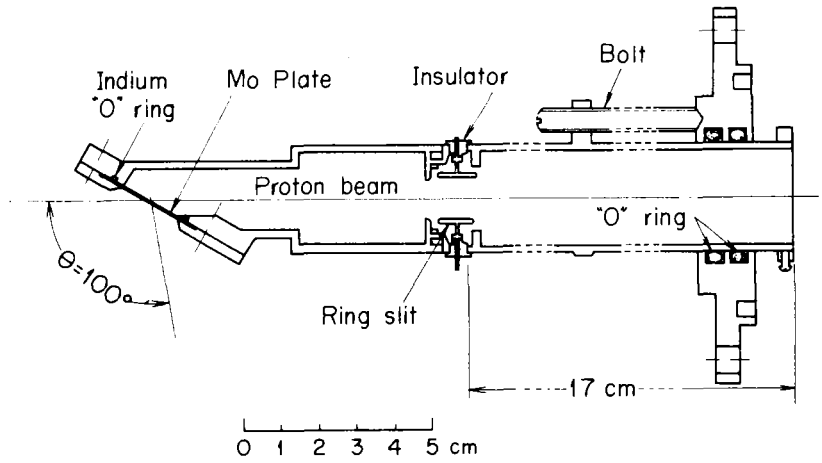

Fig. 9 100°-lithium target assembly.

II. Thickness of the lithium targets.

The rise-curve method[6] at threshold was used to determine the target thickness. The excitation curves of neutron yield of the lithium targets were measured by using a long counter from the threshold to first knee or maximum of the neutron yield. A typical result of the neutron-yield curve is shown in Fig. 10(a). The long counter was of a standard type and placed at a distance of 2.39 m from the target in the direction of $\theta = 0^{\circ}$. The thickness of lithium targets corresponding to ΔE_p was determined by the rise-width (Δf) of the neutron-yield curve obtained.

Another method[7] based on the time-of-flight technique was used for the determination of thickness of the lithium target. In order to make the detector sensitive to neutrons, an aluminum can containing 92.2% enriched ^{10}B powder of 165 gr was placed at the front of a 17 cc Ge(Li) detector. The system of the Ge(Li) detector had been assembled for the measurement of (n,n'γ) reaction, and was used in the present work for convenience.

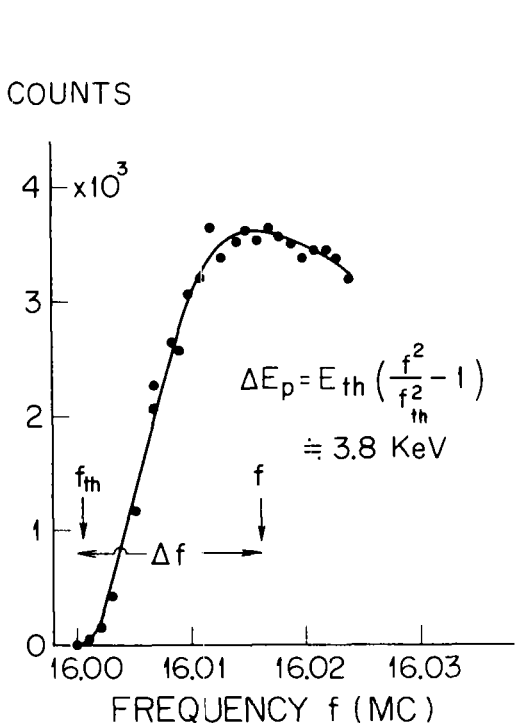

Fig. 10(a) Determination of ΔE_p by the neutron-yield curve.

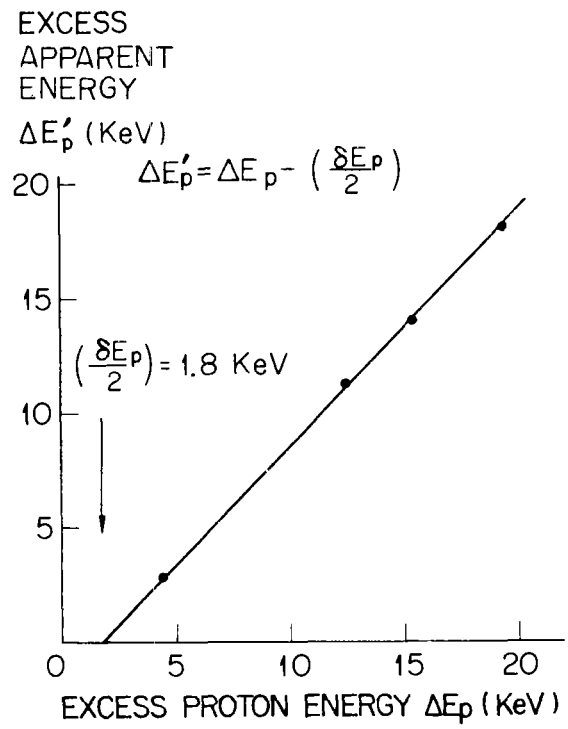

Fig. 10(b) Determination of δE_p by the time-of-flight technique.

With this time-of-flight system, the fast and slow neutron groups and gamma rays from the target were observed at 0^o direction. A typical time spectrum obtained is shown in Fig. 11. From the centroids of these three peaks, quantity of $(K_\gamma - K_f)/(K_\gamma - K_s)$ was obtsined; here K_γ , K_f and K_s are channel number of the three peaks as shown in Fig. 11. Then, the proton energy E_p' at the half-way in the target thickness, which corresponds to the energy for the quantity of $(K_\gamma - K_f)/(K_\gamma - K_s)$, was determined by the $^7Li(p,n)^7Be$ reaction kinematics.

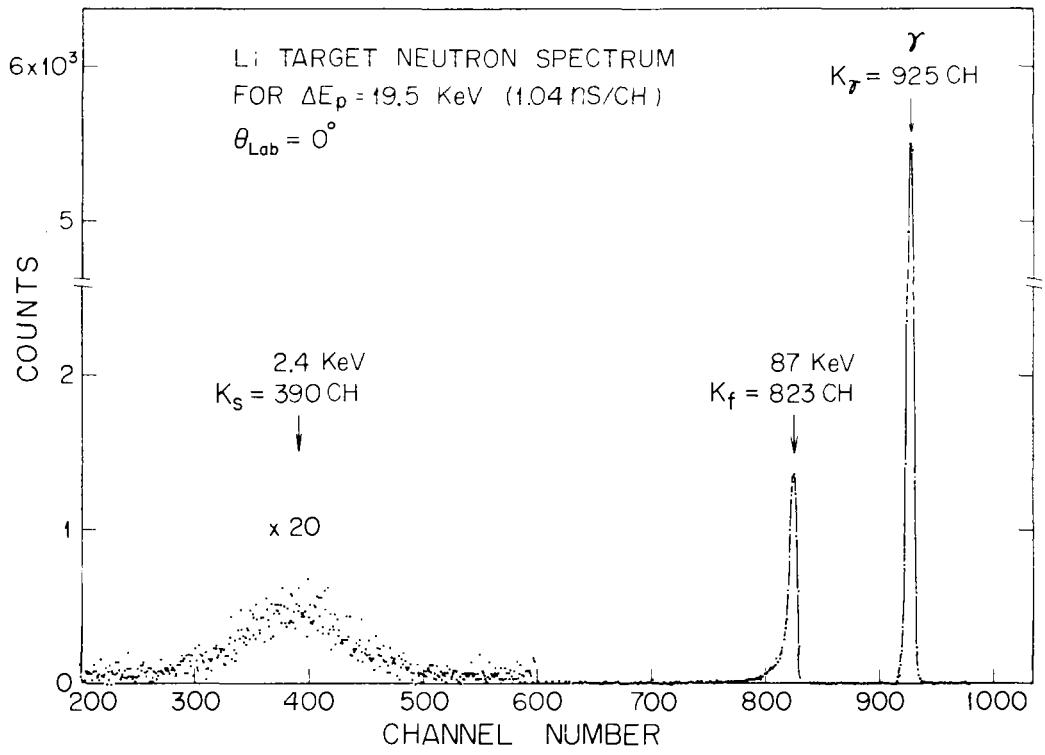

Fig. 11 Time-of-flight spectrum.

Apart from the above measurement, incident proton energy E_p hitting at the front of the target was determined by measuring the threshold energy of the $^7Li(p,n)^7Be$ reaction. By taking the difference between E_p and E_p', target thickness δE_p was deduced; i.e. $E_p - E_p' = \delta E_p/2$.

Actually, instead of using the corresponding (apparent) proton energy E_p' and the incident proton energy E_p, excess apparent proton energy $\Delta E_p'$ above the threshold and excess (incident) proton energy ΔE_p above the threshold were used. Accordingly, $E_p - E_p' = \delta E_p/2$ turned into the following formula : $\Delta E_p' = \Delta E_p - \delta E_p/2$. This formula of $\Delta E_p'$ has a linear dependence with its differential coefficient equal to +1. Therefore, the intercept on the horizontal axis (ΔE_p) gave the half value of the target thickness $\delta E_p/2$, as shown in Fig. 10(b). In Fig. 10(b), a typical result is plotted for a series of measurement at four different energy protons incident on the "3.6 keV" target.

The estimation of the lithium target thickness based on the above two different methods was in good agreement. For example, the target thickness of 3.8 keV obtained by the rise-curve method [Fig. 10(a)] was agreed to the target thickness of 3.6 keV obtained by the time-of-flight technique [Fig. 10(b)] within experimental error of about 5%.

III. Dimensions of the A-B section of the detector assembly and the polyethylene scatterer, which are shown in Fig. 1, are presented in datail in Figs. 12 and 13, respectively.

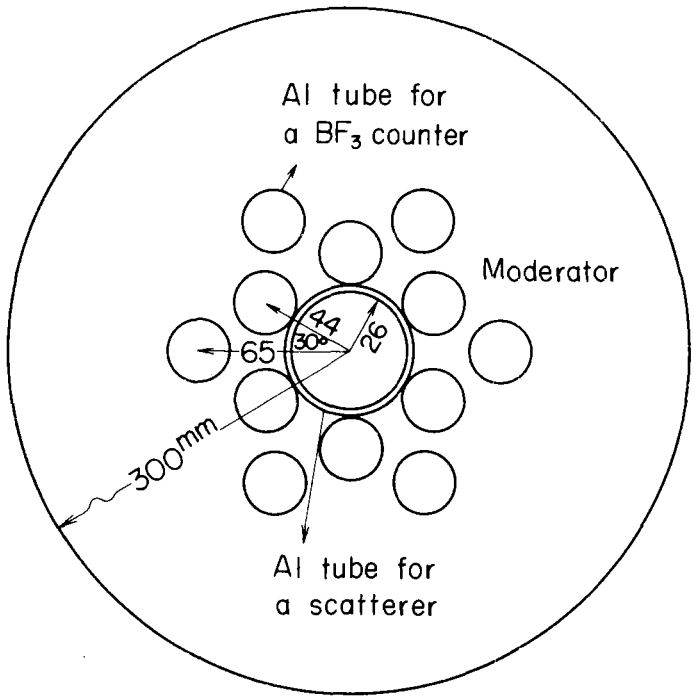

Fig. 12 A-B section of the detector assembly.

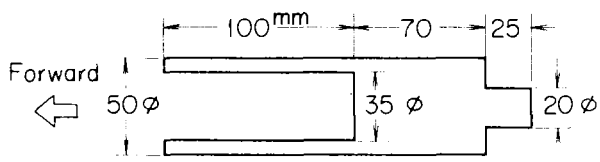

Fig. 13 Polyethylene scatterer.

いばらき印刷納